

Supplementary Information

A linear $\text{CH}^+-\text{NO}_3^-$ Base Pair Motif promoted by AgNO_3
mediated Proton Transferring between Guanosine and Cytidine

*Qiong Wu^{*a-c}, Yingying Chai^{*a-c}, Ridong Huang^{*a-c}, Hai Chen^{a-c}, Yang He^{#a-c}*

Correspondence to: Yang He, heyangqx@scu.edu.cn

Experimental Section

General methods and materials

All reagents were commercially available and used directly without further purification. The ultrapure water used in this work was produced by RODI-220B1. The SMZ18 stereoscopic microscope was used to observe the morphological characteristics of the crystals in the semi-transparent gel materials, and NIS-Elements F 4.60.00 software was used to record the images.

Crystallization of [C-Ag][NO₃]

Preparation of C/AgNO₃ complex: A 300 μ L aqueous AgNO₃ solution (0.05 M) was added to a glass vial containing solid C (1.2 mg) under light protection. A clear solution was obtained immediately with no evidence of hydrogel formation. This solution was brought to 85 °C in a water bath for 5 min and used for further investigations. C/AgNO₃ didn't form a hydrogel and remained as a clear solution.

[C-Ag][NO₃]: C/AgNO₃ aqueous solution was slowly evaporated without the exposure to light under the ambient conditions. Before the complete evaporation of the water, colorless crystalline needles were obtained within weeks, during which time the solution color became brownish with appearance of some black precipitates. The yield of crystals was 59%. ¹H NMR (400 MHz, DMSO-*d*₆) δ 8.15 (s, 1H), 8.07 (d, *J* = 7.5 Hz, 1H), 7.75 (s, 1H), 5.97 (d, *J* = 7.5 Hz, 1H), 5.81 (d, *J* = 4.3 Hz, 1H), 5.37 (s, 1H), 5.10 (s, 1H), 3.97 (dt, *J* = 14.4, 4.9 Hz, 2H), 3.86 (q, *J* = 3.3 Hz, 1H), 3.67 (dd, *J* = 12.1, 3.2 Hz, 1H), 3.57 (dd, *J* = 12.0, 3.3 Hz, 1H). ESI-MS ([C-Ag]⁺, C₉H₁₃AgN₃O₅) Calculated: 349.9906, Experimental: 349.9894 (m/z); ESI-MS ([C-Ag-C]⁺, C₁₈H₂₆AgN₆O₁₀) Calculated: 593.0761, Experimental: 593.0756 (m/z). Elemental Analysis ([C-Ag][NO₃]) Calculated : C, 26.17%; H, 3.17%; N, 13.56%; Experimental: C, 26.63%; H, 2.94%; N, 13.29%.

Crystallization of CH⁺-NO₃⁻

Preparation of G/C/AgNO₃ complex: A 300 μ L aqueous solution of AgNO₃ (0.05 M) was added to a glass vial containing the equimolar amount of G (1.4 mg) and C (1.2 mg) mixture, protected from light. The liquid mixture was rapidly converted into a clear viscous solution by gentle shaking. The resulting solution was heated in a water bath to 85°C for 5 minutes, at which temperature the hydrogel was already formed. For further experiments, the hydrogel was reheated to 95 °C, which resulted in a clear solution.

CH⁺-NO₃⁻: The G/C/AgNO₃ hydrogel was kept at room temperature and allowed to evaporate in an open vial slowly under ambient conditions without the exposure to light. The colorless crystalline needles suitable for synchrotron radiation analysis were obtained after the evaporation of the embedded water within weeks. Due to the complete embedment of the CH⁺-NO₃⁻ in the hydrogel, the total yield of the crystals could not be measured separately. ESI-MS (CH⁺, C₉H₁₄N₃O₅) calculated: 244.0933, Experimental: 244.0922 (m/z).

The structure determination of [C-Ag][NO₃] and CH⁺-NO₃⁻

Two crystals were measured at 100K during X-ray diffraction data collection using the beamline BL17B1 at the Shanghai Synchrotron Radiation Facility (Shanghai, China). The diffraction images were indexed and integrated using Olex2 ¹.

Crystal data and structure refinement parameters for CH⁺-NO₃⁻: C₉H₁₄N₃O₅, NO₃; M_r = 306.24 g·mol⁻¹; crystal size = 0.02 × 0.03 × 0.1 mm; monoclinic, space group P 2₁; a = 7.7120(5) Å, b = 7.4810(15) Å, c = 11.062(2) Å; α = 90°, β = 108.44(3)°, γ = 90°; V = 605.4(2) Å³; Z = 2; calc density = 1.680 g·cm⁻³; $F(000)$ = 320.0; T = 100K; R_{int} = 0.0000; μ = 0.107 mm⁻¹; miller index ranges, $-10 \leq h \leq 10$, $-9 \leq k \leq 9$, $-14 \leq l \leq 14$; θ_{max} = 27.840°, θ_{min} = 1.94°; T_{min} = 0.995, T_{max} = 0.997; 2869 reflections collected; 1544 independent reflections; data/restraints/parameters: 1531/0/202; goodness-of-fit on F^2 = 1.075; R_1 = 0.0311, wR_2 = 0.0843; largest diff. peak and hole: 0.22 eÅ⁻³ and -0.26 eÅ⁻³; CCDC numbers: 2150373.

Crystal data and structure refinement parameters for [C-Ag][NO₃]: C₉H₁₃AgN₄O₈; M_r = 413.10 g·mol⁻¹; crystal size = 0.08 × 0.02 × 0.01 mm; orthorhombic, space group P 2₁ 2₁ 2₁; a = 4.6969(3) Å, b = 15.1122(11) Å, c = 17.3305(12) Å; α = 90°, β = 90°, γ = 90°; V = 1230.13(15) Å³; Z = 4; calc density = 2.231 g·cm⁻³; $F(000)$ = 824.0; T = 100K; R_{int} = 0.0526; μ = 1.800 mm⁻¹; miller index ranges, $-5 \leq h \leq 5$, $-18 \leq k \leq 18$, $-21 \leq l \leq 21$; 2θ range for data collection/° 5.56 to 53.522; T_{min} = 0.007, T_{max} = 0.023; 16250 reflections collected; 2401 independent reflections; data/restraints/parameters: 2401/0/202; goodness-of-fit on F^2 = 1.104; R_1 = 0.0358, wR_2 = 0.1139; largest diff. peak and hole: 0.96 eÅ⁻³ and -0.68 eÅ⁻³; CCDC numbers: 2150374.

Preparation of G/AgNO₃ complex:

A 300 µL aqueous AgNO₃ solution (0.05 M) was added to a glass vial containing the G (1.4 mg) under light protection. A hydrogel with some undissolved G dispersed was then rapidly formed. The resulting hydrogel became a clear solution when heated to 67 °C. The clear solution was brought to 85 °C for 5 min in a water bath for further studies. The G/AgNO₃ complex solution at 85 °C was brought to room temperature under ambient conditions, which again turned into solidified hydrogel.

When 1.4 mg G was added to the preformed C/AgNO₃ solution (1.2mg C in a 300 µL aqueous 0.05 M AgNO₃ solution), the same G/C/AgNO₃ hydrogel system could be obtained as the simultaneous addition of three components together. In addition, the [C-Ag][NO₃] solid complex (6.1 mg) with same structure as [C-Ag][NO₃] single crystals were dissolved, and then the G (1.4 mg) was added into this [C-Ag][NO₃] clear solution, which also lead to a same hydrogel phenomena as G/C/AgNO₃.

Preparation of solid complexes of G/AgNO₃, C/AgNO₃ and G/C/AgNO₃

The corresponding solution complexes of G/AgNO₃, C/AgNO₃ and G/C/AgNO₃ were prepared and were dried by evaporation at room temperature under the protected of light.

Calculations

For the crystallographic complexes, the fragments were extracted from their crystal structure. The DFT (B3LYP)/def2tzvp level with D3 dispersion correction was used with Boys-Bernardi counterpoise correction for the interaction energy calculation. In addition, the solvation energy of each species in water was used with Solvation Model Based on Density (SMD) method implemented in Gaussian.

Hirshfeld surface analysis and 2D fingerprint plots were used by CrystalExplorer-21.5 to visualize the holistic interactions.⁴ Input files of IGMH were obtained from Gaussian calculation results, and IGMH images were calculated by Multiwfn 3.8.⁵ The resulting cube files from Multiwfn 3.8 were visualized by VMD 1.9.3 program.⁶

The cryo-SEM measurements

For the cryo-SEM measurements, 10 μL of G/AgNO_3 , C/AgNO_3 and G/C/AgNO_3 complex solutions and the corresponding dilutions (1:10, 1.67 mM) were used. For the high concentration, C/AgNO_3 (167 mM), saturated G/C/AgNO_3 was used, and G/AgNO_3 were not measured due to its poor solubility.

For the measurements, the sample stage was pre-cooled to -20°C first and 10 μL hot solutions were added to the concave surface of the sample holder. After the sample was completely frozen, the vacuum pump was started and the SEM images were recorded using the semiconductor backscattered-electron (BE) detector at different magnifications with a Zeiss EVO10.

Scanning Electron Microscopy (SEM)

The 20 μL of samples of G/AgNO_3 , C/AgNO_3 and G/C/AgNO_3 were placed in the $5\times 5\times 2\text{mm}$ sample holders, and the solids of G/AgNO_3 , C/AgNO_3 and G/C/AgNO_3 complexes dried at room temperature were used for SEM measurements using a common secondary electron (SE) detector of Zeiss EVO10.

TEM measurements

The complexes of G/AgNO₃, C/AgNO₃ and G/C/AgNO₃ were diluted to 1:100 (167 μM) and 1:3000 (5.56 μM), and heated in a water bath at 85°C for 5 minutes. Then, the solution was cooled to room temperature and stored for 2 days in the absence of light. A 10 μL aliquot of these solutions was applied to perforated carbon-coated copper grids, and the excess liquid was blotted off. The grids were then dried at room temperature in the absence of light. The dried samples on the grids were sent to the FEI Tecnai G2 S-Twin F20 Microscope for transmission electron microscope (TEM) imaging.

PXRD measurements

The G/AgNO₃, C/AgNO₃ and G/C/AgNO₃ solid complexes were prepared according to the above-mentioned procedures. And these samples were measured by Rigaku D/Max 2250 V/PC X-ray diffractometer with Cu Kα radiation ($\lambda=1.54056\text{\AA}$) at 50 KV and 200 mV in the angle range of $5^{\circ}\leq 2\theta\leq 90^{\circ}$ to record the powder X-ray diffraction (PXRD) signals at room temperature.

NMR experiments

The G, C, G/C and their solid complexes of C/AgNO₃, G/AgNO₃ and G/C/AgNO₃ were dissolved in *d*₆-DMSO, and the ¹H NMR and the temperature varying experiments from 25°C-85°C were measured.

Mass Spectra measurements

The crystals of [C-Ag][NO₃] and CH⁺-NO₃⁻ were dissolved and diluted into 16.5 μM, and 20 μL of the diluted solutions for each complex were used for mass spectra measurements using ThermoScientific Q Exactive.

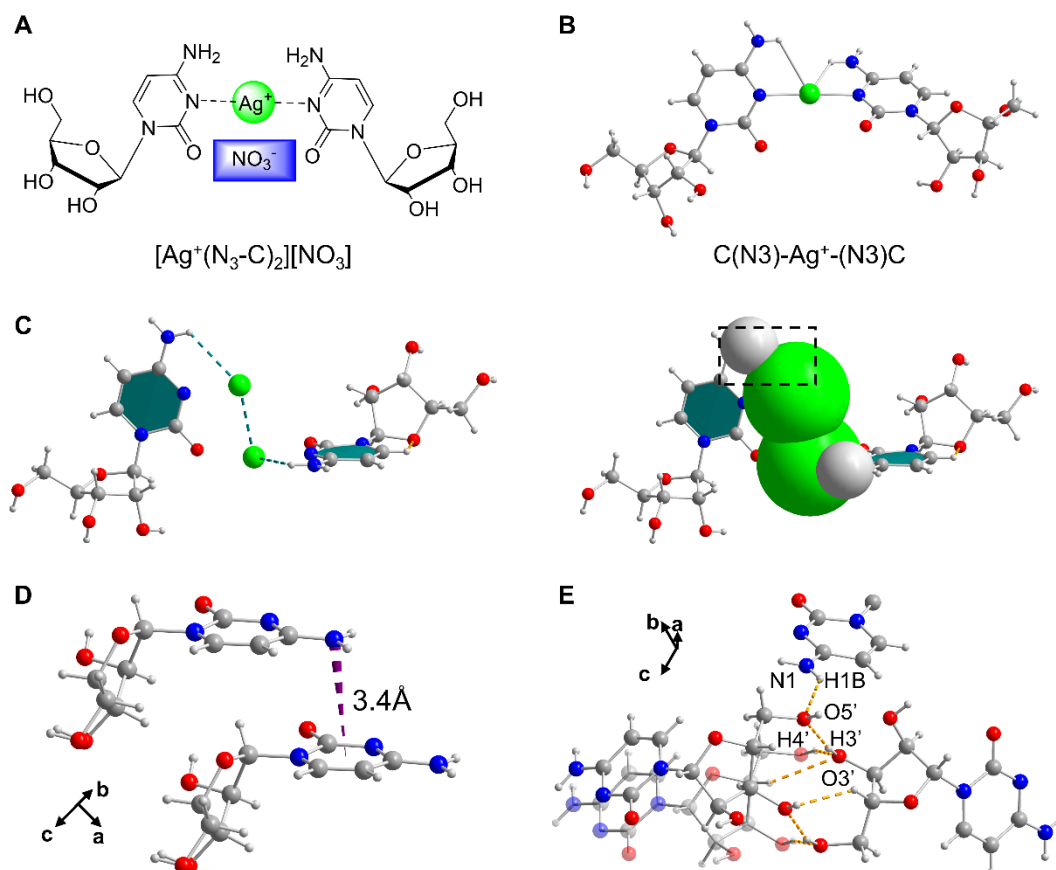


Figure S1. The detailed depiction of molecules **1** and $[\text{Ag}^+(\text{N}_3\text{-C})_2][\text{NO}_3]$. (A) The chemical structure of $[\text{Ag}^+(\text{N}_3\text{-C})_2][\text{NO}_3]$; (B) The $[\text{Ag}^+(\text{N}_3\text{-C})_2][\text{NO}_3]$ structure of motif **C(N3)-Ag⁺-(N3)C**; (C) The ball-stick and space-filling model of $\text{Ag}^+\cdots\text{H}_8\text{-N}_4$ in **1**; (D) The N- π stacking between the two neighbored molecules; (E) The hydrogen bonds between the adjacent sugar residues.

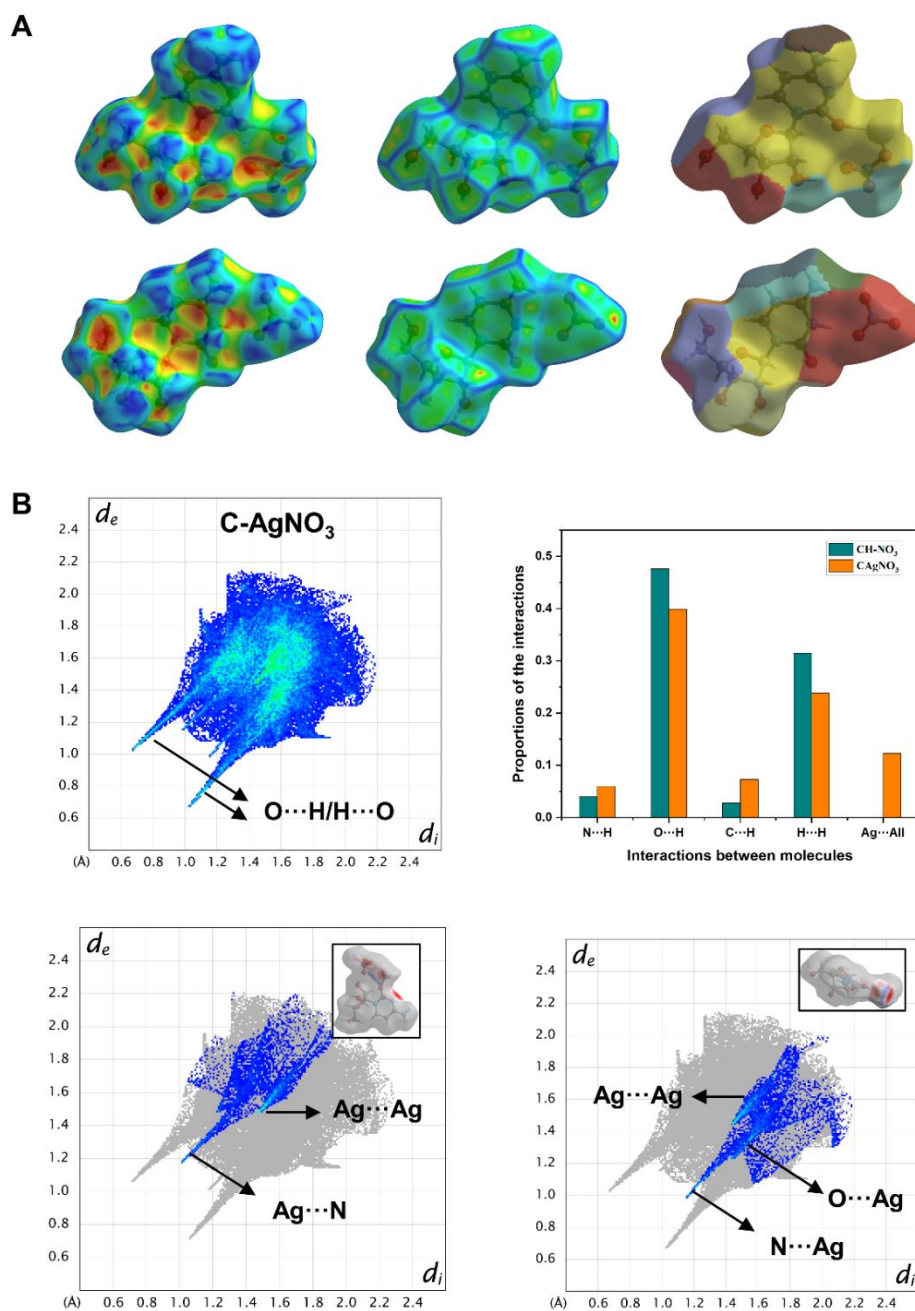


Figure S2. The Hirshfeld surface analysis of molecules 1 and 2. (A) The curvedness, shapeindex and segments of 1 and 2; (B) The 2D Fingerprint plots analysis of 1.

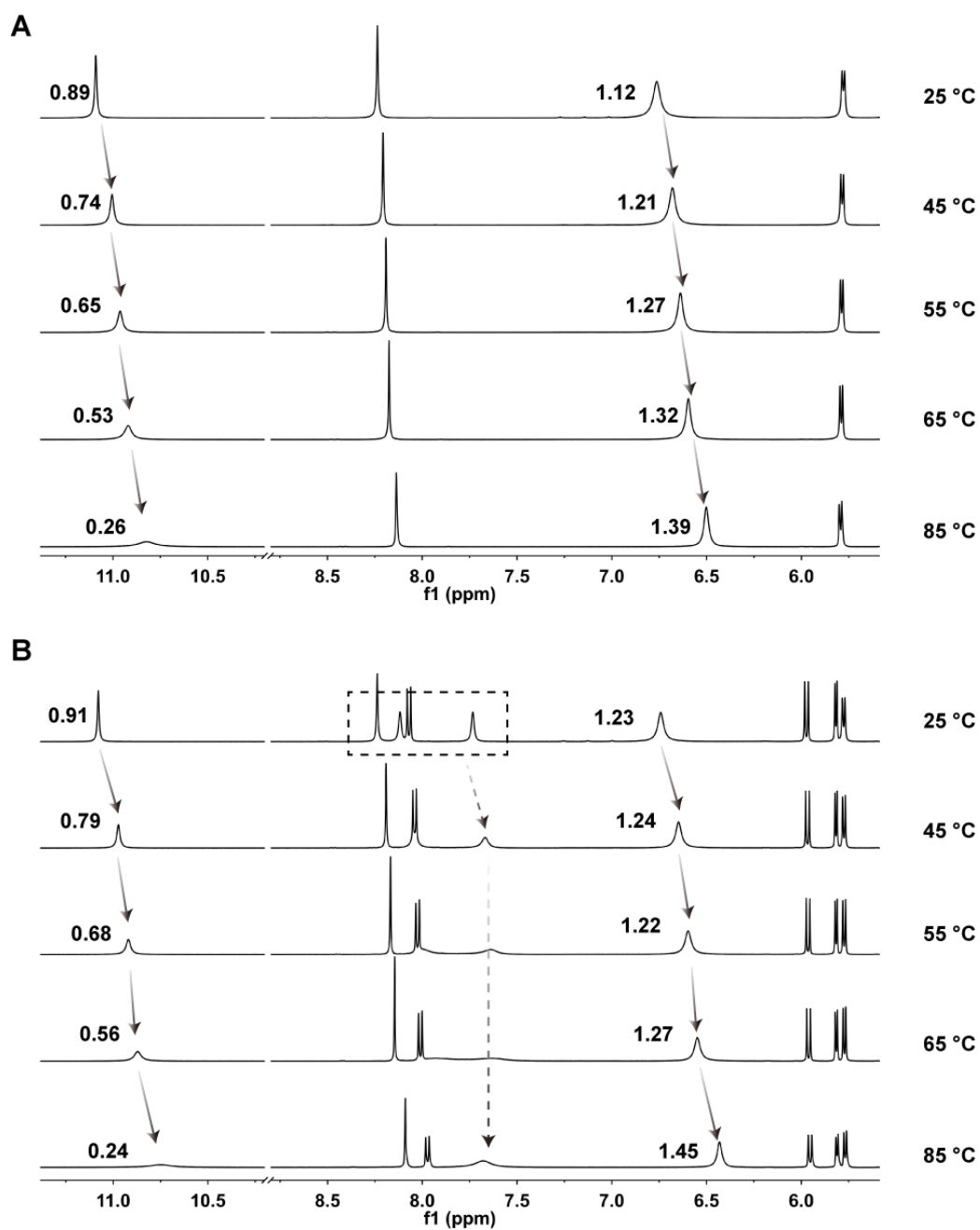


Figure S3. The ^1H NMR temperature varying experiments of G/AgNO_3 (A) and $\text{G}/\text{C}/\text{AgNO}_3$ (B) from 25°C to 85°C.

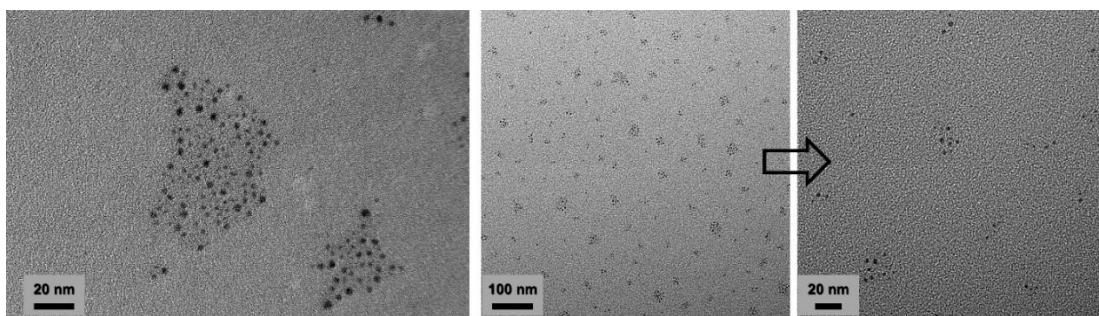


Figure S4. TEM images of the C/AgNO₃. TEM image of 5.56 μM C/AgNO₃ (left), and 167 μM C/AgNO₃ (middle) and its magnification images (right).

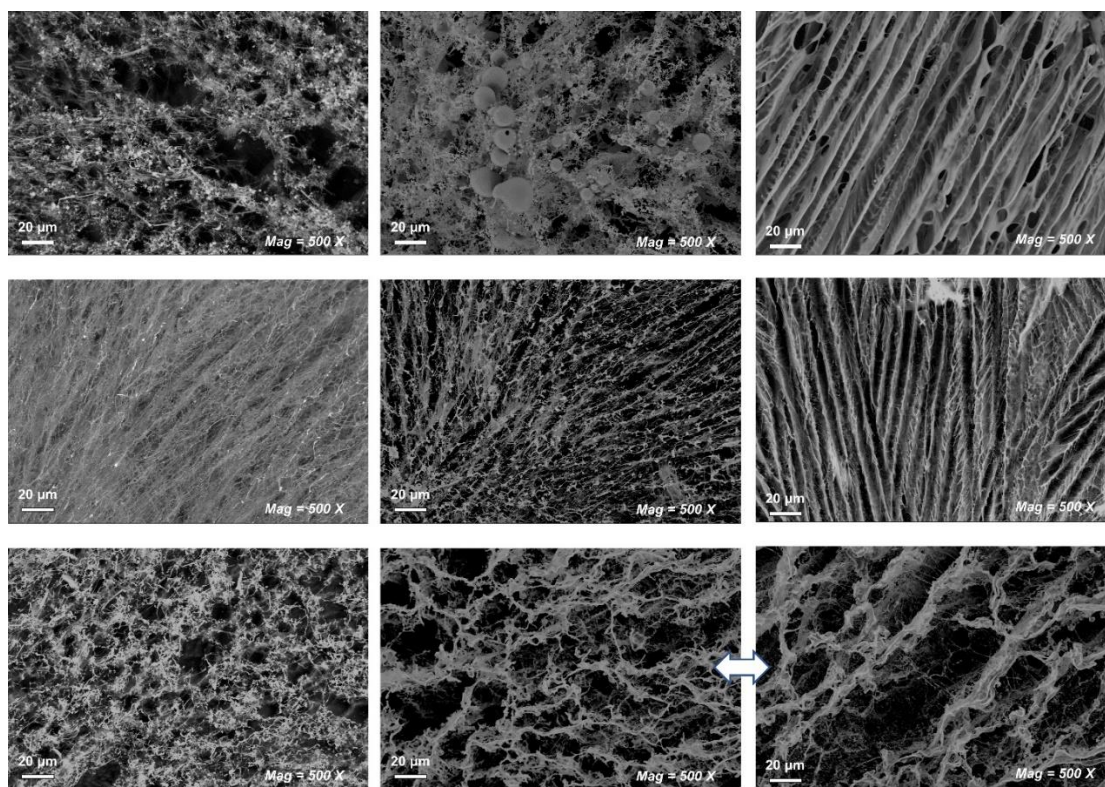


Figure S5. Cryo-SEM images of the C/AgNO₃, G/C/AgNO₃ and G/AgNO₃. Cryo-SEM image of 1.67 mM **C/AgNO₃** (left upper), **G/C/AgNO₃** (left middle) and **G/AgNO₃** (left bottom); Cryo-SEM image of 16.7 mM **C/AgNO₃** (middle upper), **G/C/AgNO₃** (middle middle) and **G/AgNO₃** (middle bottom and right bottom); Cryo-SEM image of 167 mM **C/AgNO₃** (right upper), saturated **G/C/AgNO₃** (right middle).

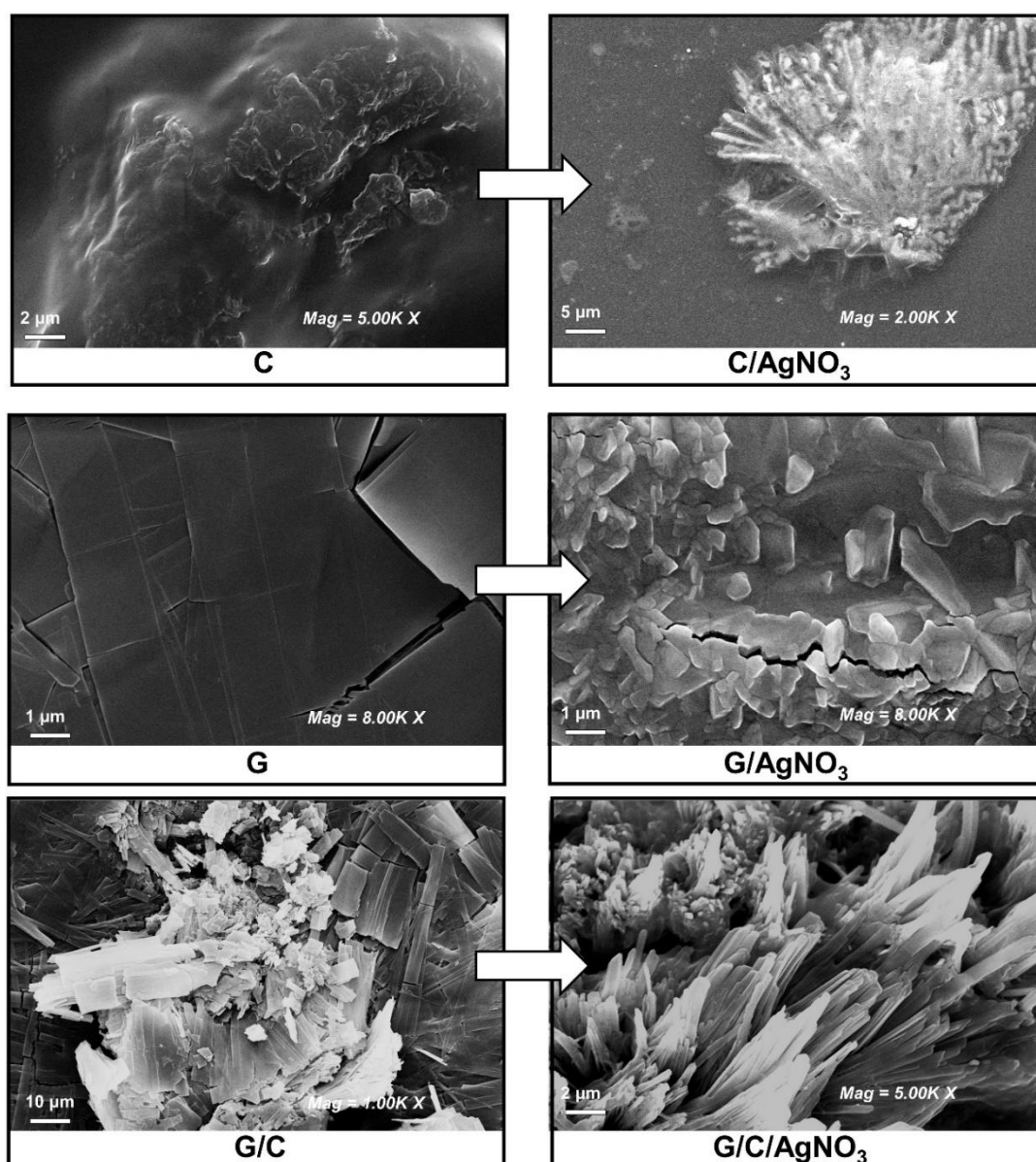


Figure S6. The SEM characterizations of G, C, G/C and their Ag-complexes in solid states. The SEM images of C, G and G/C in solid states (left) and SEM images of C/AgNO₃, G/AgNO₃ and G/C/AgNO₃ in solid states (right).

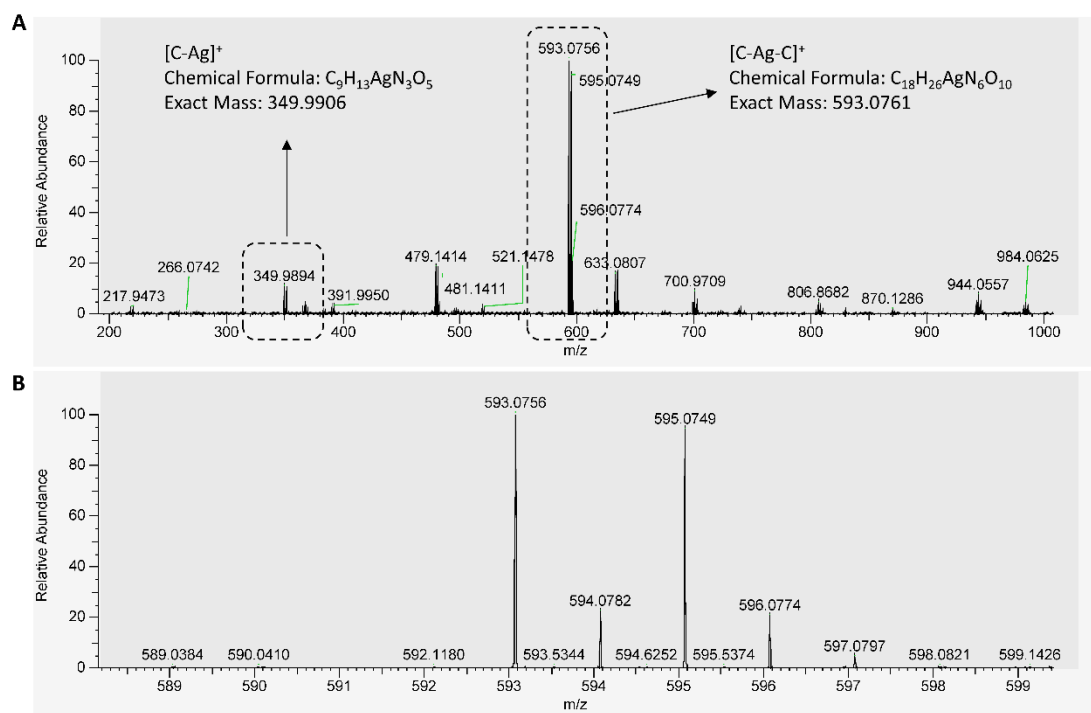


Figure S7. The ESI-MS spectra of $[C-Ag][NO_3]$ collected in high resolution positive ion mode. (A) The full mass spectra of $[C-Ag][NO_3]$ with the $C-Ag^+$ complex and $C-Ag^+-C$ base pair motif observed. (B) The mass spectra of $C-Ag^+-C$ with the detail isotope of Ag.

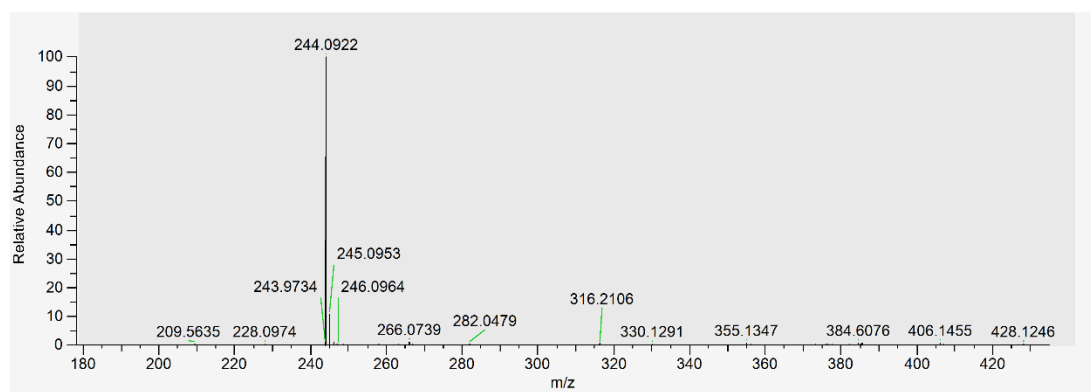


Figure S8. The ESI-MS spectra of $\text{CH}^+\text{-NO}_3^-$ collected in high resolution positive ion mode. Only the $[\text{CH}]^+$ peak with the chemical formulation of $\text{C}_9\text{H}_{14}\text{N}_3\text{O}_5$ was observed.

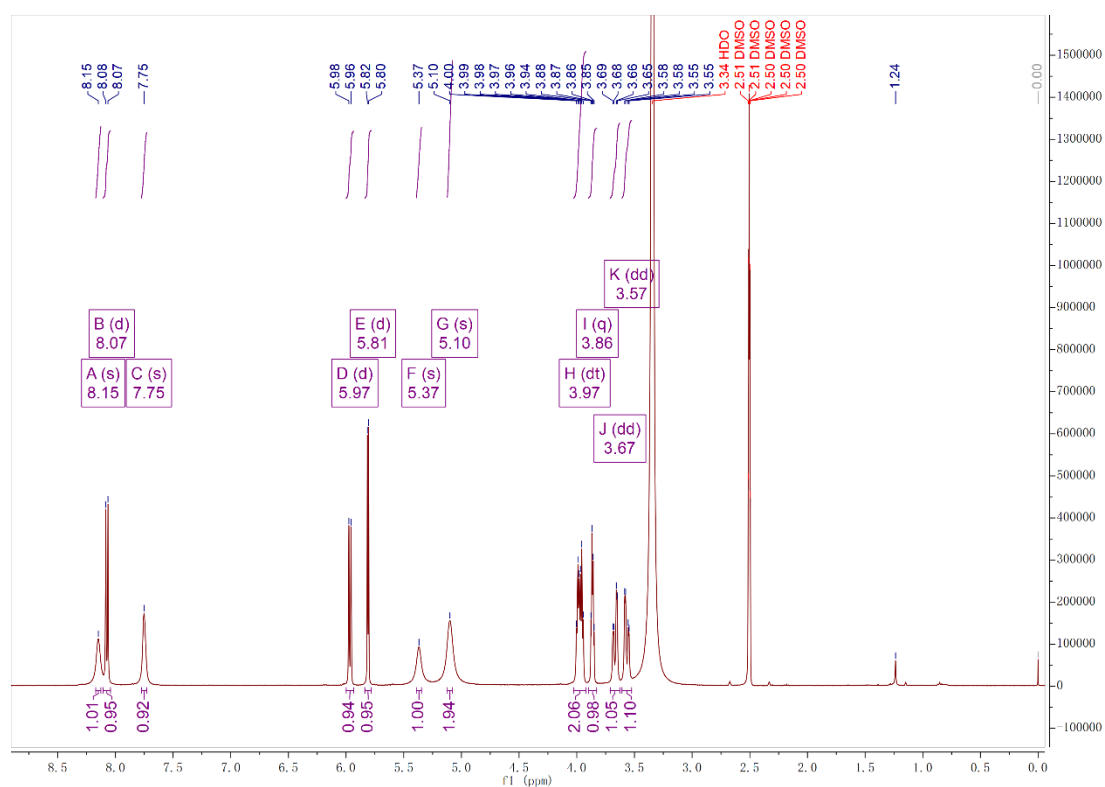


Figure S9. The ^1H -NMR spectrum of $[\text{C-Ag}][\text{NO}_3]$.

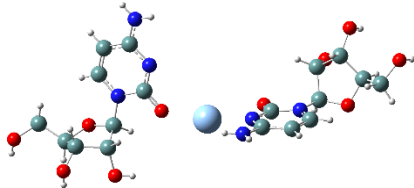
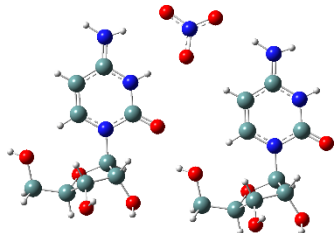
Table S1. Hydrogen bond lengths (Å) and bond angles (°) for [C-Ag][NO₃].

| | D-H...A | d(D-H) / Å | d(H...A) / Å | d(D...A) / Å | Angles D-H...A / ° |
|------------------------------------|----------------|------------|--------------|--------------|-----------------------|
| hydrogen bond | N4-H4A...O1 | 0.88 | 1.99 | 2.831(8) | 160 |
| | N4-H4B...O5' | 0.88 | 2.29 | 2.957(8) | 133 |
| | O3'-H3''...O5' | 0.84 | 1.95 | 2.773(7) | 167 |
| | O5'-H5'...O3' | 0.84 | 1.93 | 2.737(7) | 160 |
| | C4'-H4'...O3' | 1.00 | 2.59 | 3.342(9) | 132 |
| Intro- molecular interaction | O2-H2'...O3 | 0.84 | 1.96 | 2.784(8) | 168 |
| | C6-H6...O4' | 0.95 | 2.35 | 2.707(9) | 101 |
| | C1'-H1A'...O3 | 1.00 | 2.54 | 3.538(10) | 176 |

Table S2. Hydrogen bond lengths (Å) and bond angles (°) for CH⁺-NO₃⁻

| | D-H...A | d(D-H) / Å | d(H...A) / Å | d(D...A) / Å | Angles D-H...A / ° |
|------------------------------------|-----------------|------------|--------------|--------------|-----------------------|
| Strong hydrogen bond | N4-H4A...O3 | 0.84 | 2.10 | 2.935(3) | 174 |
| | N4-H4B ...O4 | 0.98(5) | 2.03(5) | 3.013(3) | 178(4) |
| | N3-H3...O1 | 0.84(4) | 1.87(4) | 2.713(2) | 174(3) |
| | O2'-H2''...O3 | 0.84 | 2.14 | 2.951(2) | 162' |
| | O3'-H3'' ...O5' | 0.84 | 1.91 | 2.748(2) | 173 |
| | O5'-H5''...O2 | 0.84 | 2.20 | 2.887(2) | 139 |
| | O5'-H5''...O2' | 0.84 | 2.56 | 3.031(2) | 117' |
| Weak hydrogen bonds | C5-H5...O1 | 0.95 | 2.31 | 3.240(3) | 168 |
| | C2'-H2'...O4 | 1.00 | 2.54 | 3.379(2) | 141 |
| | C4'-H4'...O2' | 1.00 | 2.58 | 3.343(2) | 133 |
| | C5'-H5B'...O4 | 0.99 | 2.43 | 3.359(3) | 157 |
| Intro- molecular interaction | O2'-H2'' ...O3' | 0.84 | 2.35 | 2.744(2) | 110 |
| | C6-H6...O4' | 0.95 | 2.36 | 2.700(3) | 100 |
| | C6-H6...O5' | 0.95 | 2.27 | 3.153(3) | 155' |
| | C3'-H3'...O5' | 1.00 | 2.55 | 2.960(3) | 104 |

Table S3. Base pairs and the corresponding complexes energy

| Base pairs type | Base pair structures | Complexes Energy |
|-----------------|---|---------------------------------------|
| Motif I |  | $\Delta E = -112.03 \text{ kcal/mol}$ |
| Motif II |  | $\Delta E = -135.83 \text{ kcal/mol}$ |

References of Support Materials:

1. O. V. Dolomanov, L. J. Bourhis, R. J. Gildea, J. A. K. Howard and H. Puschmann, *J. Appl. Cryst.*, 2009, **42**, 339-341.
2. GaussView, Version 6, R. Dennington, T. Keith, J. Millam, Semichem Inc., Shawnee Mission, KS, 2019.
3. Gaussian 09, M. J. Frisch, G. W. Trucks, H. B. Schlegel, G. E. Scuseria, M. A. Robb, J. R. Cheeseman, G. Scalmani, V. Barone, G. A. Petersson, H. Nakatsuji, X. Li, M. Caricato, A. Marenich, J. Bloino, B. G. Janesko, R. Gomperts, B. Mennucci, H. P. Hratchian, J. V. Ortiz, A. F. Izmaylov, J. L. Sonnenberg, D. Williams-Young, F. Ding, F. Lipparini, F. Egidi, J. Goings, B. Peng, A. Petrone, T. Henderson, D. Ranasinghe, V. G. Zakrzewski, J. Gao, N. Rega, G. Zheng, W. Liang, M. Hada, M. Ehara, K. Toyota, R. Fukuda, J. Hasegawa, M. Ishida, T. Nakajima, Y. Honda, O. Kitao, H. Nakai, T. Vreven, K. Throssell, J. A. Montgomery, Jr., J. E. Peralta, F. Ogliaro, M. Bearpark, J. J. Heyd, E. Brothers, K. N. Kudin, V. N. Staroverov, T. Keith, R. Kobayashi, J. Normand, K. Raghavachari, A. Rendell, J. C. Burant, S. S. Iyengar, J. Tomasi, M. Cossi, J. M. Millam, M. Klene, C. Adamo, R. Cammi, J. W. Ochterski, R. L. Martin, K. Morokuma, O. Farkas, J. B. Foresman, and D. J. Fox, Gaussian, Inc., Wallingford CT, 2016.
4. P. R. Spackman, M. J. Turner; J. J. McKinnon, S. K. Wolff, D. J. Grimwood, D. Jayatilaka and M. A. Spackman, *J. Appl. Cryst.*, 2021, **54**, 1006-1011.
5. T. Lu and F. Chen, *J. Comput. Chem.*, 2012, **33**, 580-92.
6. W. Humphrey, A. Dalke and K. Schulten, *J. Mol. Graph.*, 1996, **14**, 33-38.